

Relativity and the lead-acid battery

Rajeev Ahuja,^{1,*} Andreas Blomqvist,¹ Peter Larsson,¹ Pekka Pyykkö,^{2,†} and Patryk Zaleski-Ejgierd^{2,‡}

¹*Division of Materials Theory, Department of Physics and Astronomy,
Uppsala University, Box 516, SE-751 20, Uppsala, Sweden*

²*Department of Chemistry, University of Helsinki, Box 55 (A. I. Virtasen aukio 1), FI-00014 Helsinki, Finland*

(Dated: November 26, 2024)

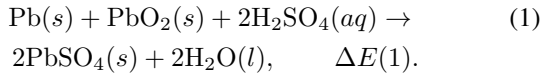
The energies of the solid reactants in the lead-acid battery are calculated *ab initio* using two different basis sets at non-relativistic, scalar relativistic, and fully relativistic levels, and using several exchange-correlation potentials. The average calculated standard voltage is 2.13 V, compared with the experimental value of 2.11 V. All calculations agree in that 1.7-1.8 V of this standard voltage arise from relativistic effects, mainly from PbO₂ but also from PbSO₄.

PACS numbers: 82.47.Cb, 82.60.Cx, 31.15.ae, 31.15.aj, 31.15.es

Keywords: lead, lead battery, relativity, relativistic effects

The lead battery is an essential part of cars, and has numerous other applications. This well-known invention is now 150 years old [1, 2]. About 75% of the World lead production and a turnover of about 30 billion USD are due to these batteries. Although there are electrochemical simulations starting from the given thermodynamical data[3, 4], we are not aware of any *ab initio* ones for the lead battery. This is in stark contrast to other rechargeable batteries, such as the modern lithium-ion based systems, where they abound. The problem is difficult enough to be a theoretical challenge, and there is the additional fascination that, Pb being a heavy-element, relativistic effects on its compounds could play an important role, as qualitatively found a long time ago[5–8]. For metallic lead, see [9–11].

The discharge reaction of the lead-acid cell is

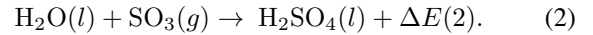


The electronic structures of both PbO[12–14] and β -PbO₂[15–17] have been theoretically studied earlier. Especially, the metallic conductivity of the β -PbO₂, making the large currents possible, was shown to be an impurity, conduction-band effect, attributed to donor impurities at oxygen sites[16–19]. The alloying of the Pb electrode is also important in practice, but is not discussed here, because the minute amounts of other elements do not affect the EMF of the cell.

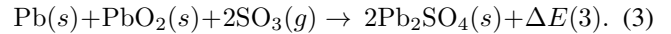
The construction of the lead-acid battery[20] has a positive lead dioxide electrode, a negative electrode of metallic lead, and a sulfuric acid electrolyte. The discharge reaction between a Pb(IV) and a Pb(0) produces 2 Pb(II), in form of solid PbSO₄. The experimental thermodynamics of the reaction are well-known[21].

The three solids can be treated with existing solid-state theories, such as density functional theory (DFT), because the bonding mechanism in the investigated species is dominated by covalent interactions where DFT is expected to provide reliable results. Adequately simulating the liquid phase in multiple relativistic regimes is beyond current state of the art, how-

ever. We avoid this problem by introducing the known energy $\Delta E(2)$ for the experimental reaction



We can use this empirical relationship because only light elements and only S(VI) occur in eq. (2), whose contribution to relativistic effects are small. Combining the equations (1) and (2) gives



The voltages for the lead-acid battery reaction may then be calculated from the reaction energies

$$\Delta E(1) = \Delta E(3) - 2\Delta E(2) \quad (4)$$

where we use calculated $\Delta E(3)$ values and experimental $\Delta E(2)$ values. Concentrated sulfuric acid is used in reactions (1) and (2). The cell voltage at typical 5.5M (in H₂SO₄·10H₂O) is calculated using the values tabulated by Duisman[21].

Prediction of formation energies in a quantitative manner from *ab initio* calculation requires, in addition to having an accurate underlying theory, also absolute convergence of all technical parameters and a sufficiently general basis set. It is therefore fruitful to approach the problem with several independent methods, and see if they converge on the result. In our case, we used a linear combination of local orbitals (LCAO), with and without a frozen core approximation, using the BAND program[22]; and a full-potential local-orbital minimum-basis approach[23] with the FPLO program (version 7.00-27).

The calculations are performed with crystal structures from experimental room-temperature measurements (for structures see the Supplementary Material), allowing no ionic relaxations, thus capturing the dynamic electronic effects of relativity (meaning Dirac vs. Schrödinger). The alternative, more laborious choice would have been to also consider the relativistic structural and vibrational changes, including zero-point energies (ZPE). The thermal effects on the reaction en-

ergies are fairly small and are simply neglected. If a battery freezes at low temperatures, it is due to the kinetics, not due to the ΔG . As stated, we assume for simplicity pure, unalloyed Pb and a pure β -PbO₂ phase in the electrode materials. The measured cell voltages for α and β -PbO₂ differ by ca. 0.01 V[24].

In the LCAO approach, the one-electron basis sets representing the optimized electron density consist of linear combination of Herman-Skillman numerical atomic orbitals (NO) and Slater-type orbitals (STO). We apply a quadruple-zeta basis sets augmented with four polarization functions (QZ4P), available in the BAND basis-set repository. Frozen-core approximation is consistently applied to reduce the size of the variational basis set. The use of frozen core, as implemented in BAND[22], is preferable over pseudopotential techniques because it essentially allows for all-electron calculations. The frozen core orbitals are taken from high-accuracy calculations with extensive STO basis sets. For oxygen and sulphur, we use all-electron basis sets. For lead we include up to 4f orbitals in the core. The slight change in the deep-core orbitals due to formation of chemical bonds was confirmed to be negligible.

The band nature of the solid-state species was inferred by studying the density of states (DOS). The orbital character of the total DOS was determined with respect to contributions from individual atoms. The band structure along a series of lines of high symmetry was also analyzed. The overall band structures change only slightly with the method: the ordering, the orbital character and the dispersion remain comparable within LDA and GGA approximations.

In the case of BAND calculations, we used experimentally determined structures both for solid- and gas-phase species. The lattice constants and atomic positions were kept fixed in all calculations, motivated by our interest in purely the electronic rearrangement effects due to relativity. The relativistic effects are investigated by means of the zeroth-order regular approximation (ZORA). We consider three cases: non-relativistic (NR), scalar relativistic (SR) and the fully relativistic (FR) with first-order spin-orbit effects taken into account. To ensure high accuracy results, the convergence of the calculations was checked with respect to all crucial numerical parameters including the number of k-points, basis set quality and size of the frozen core. The formation energies were calculated with respect to spherically symmetric spin-restricted atoms and converged within 1 kJ/mol or less. To sample the first Brillouin zone, and evaluate the k-space integrals, we used a quadratic numerical integration scheme with $9 \times 9 \times 9$ (Pb and Sn), $5 \times 5 \times 5$ (PbO, PbO₂, SnO, SnO₂) and $3 \times 3 \times 3$ (PbSO₄, SnSO₄) meshes. The SO₃ molecule was placed in the middle of a large cubic unit cell ($a=20 \text{ \AA}$) with a single k-point.

In the FPLO approach, we performed band-structure calculations using the non-relativistic, the scalar-relativistic and the full four-component relativistic versions of the full potential local orbital minimum-basis band-structure method[23] (FPLO version 7.00-27). The Local density approximation

TABLE I. Comparison of the experimental and calculated results for the EMF [V] of the lead-battery reaction (1).

Method	Level of relativity			Δ	Δ
	NR	SR	FR		
BAND VWN	+0.55	+2.52	+2.27	+1.72	+1.97
	PBEsol-D	+0.21	+2.25	+2.02	+1.81
FPLO PW92	+0.41	+2.20	+2.10	+1.69	+1.80
	PW92b	+0.39	+2.21	+2.11	+1.72
Av.	+0.39	+2.30	+2.13	+1.74	+1.91
Exp. ^a			+2.107		

^a Ref. [24]

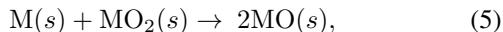
was used[25] for the exchange-correlation functional. Here, the optimal volumes of the crystal structures were determined by calculating the experimentally determined structures at different volumes and fitting a 4th-order polynomial equation of state to the data points. To sample the first Brillouin zone and evaluate the k-space integrals we use a linear numerical integration scheme with $24 \times 24 \times 24$ (Pb and Sn), $12 \times 12 \times 12$ (PbO, PbO₂, SnO, SnO₂) and $6 \times 6 \times 6$ (PbSO₄, SnSO₄) k-point meshes. The SO₃ molecule was calculated without periodic boundary conditions.

The resulting reaction energies for the lead battery reaction(1), calculated at the FR (fully relativistic), SR (scalar relativistic = without spin-orbit coupling), and NR (non-relativistic) levels are compared to experiment in Table I. We manage to reproduce the absolute voltage of the lead battery reaction within about 0.2V. Taking the four calculations in Table I at face value, our calculated absolute voltage for reaction (1), in H₂SO₄·10H₂O, is +2.13 V while its relativistic part is +1.74 V. The relativistic increase of the oxidative power of β -PbO₂(s) is indeed the largest contribution. The PbSO₄(s) contribution to EMF follows, and has the same sign. The third largest contribution comes from the spin-orbit coupling effects in metallic Pb. At 'PBEsol-D' level of theory these three contributions are +1.58, +0.27 and -0.06 V, respectively, and were seen to be essentially method-independent. For details on individual contributions, see Fig. 1.

Comparing Pb with its lighter congener Sn, it has been noticed before that no corresponding 'tin battery' exists[26]. This was attributed to the lower oxidative power of tin dioxide, as compared to lead dioxide. We find support for this conclusion in our calculations, since a tin battery would roughly correspond to a lead battery without relativistic effects (see below). Indeed we found the largest relativistic shifts in the lead dioxide. In Fig. 2 we show the FR, SR, and NR densities of states (DOS) of Pb in β -PbO₂(s). We see that the Pb 6s character is evenly distributed between the filled and empty states[16], making this shell "half-oxidized". Furthermore, the size of the band gap decreases with increasing level of relativity (NR, SR, FR). Note also the relative shifts and

changes in the Pb 6s population at different levels of relativity. The Pb 6s states are significantly stabilized by inclusion of relativity also in β -PbO₂.

We derived above the cell voltage of reaction (1) by using a combination of experimental and theoretical results. In order to validate the solid-state DFT part - something which cannot be taken for granted - we also considered the simplified 'toy model' reactions, taking place entirely in the solid-state,



with M being Pb or Sn. The reaction energy of this model can be calculated completely by DFT, and should be close to experiment. We find that this is the case, with the voltages for Pb being within 0.05 V of the experimental value for the two different DFT implementations and several different exchange-correlation functionals, see Fig. 3. This suggests that our theoretical calculations accurately describe reality. In Fig. 1, we show the calculated energies of formation, E_f , of individual species at various levels of relativity. The relativistic shift is most pronounced for solid β -PbO₂. For solid PbO it is approximately five times smaller and has the same sign. In the case of the tin 'toy-model', the largest relativistic contribution arises from SnO₂, followed by SnO and Sn, for which the relativistic shifts are only slightly different.

Returning to a qualitative discussion, we mean here by relativistic effects anything that depends on the speed of light or, more technically, the results of the Dirac versus Schrödinger one-electron equation. The main effects are the stabilization of all *ns* and *np* shells, the destabilization of the *nd* and *nf* shells and the spin-orbit (SO) splitting of the *p,d,f, ...* shells. For example, the fully relativistic (FR) and non-relativistic (NR) atomic orbital energies of tin and lead are shown in Fig. 4. As noticed before[7, 8], the non-relativistic values

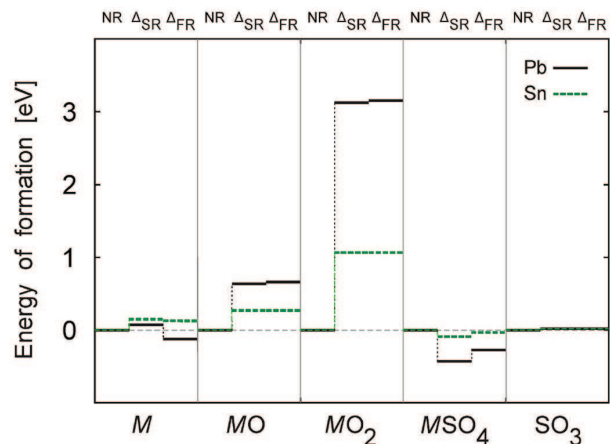


FIG. 1. The relativistic shifts in energies of formation, E_f (per formula unit), calculated at DFT/PBESol-D level. The non-relativistic energy, NR = $E_f(\text{NR})$, is chosen as reference; $\Delta_{\text{SR}} = E_f(\text{SR}) - E_f(\text{NR})$, and $\Delta_{\text{FR}} = E_f(\text{FR}) - E_f(\text{NR})$. Note the smallness of the effect on SO₃(g).

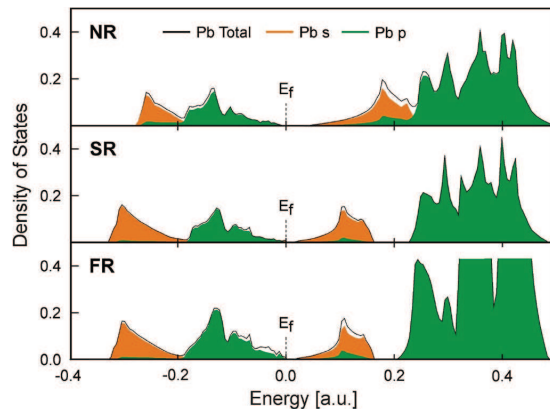


FIG. 2. Total and partial DOS (states/eV/cell) of Pb in β -PbO₂ calculated at DFT/VWN level (the Fermi energy, E_F , is set to 0). Note the pronounced relativistic shift in both occupied and unoccupied Pb 6s-states. (NR - non-relativistic, SR - scalar-relativistic, FR - fully-relativistic). Orange: Pb 6s, green: Pb 6p.

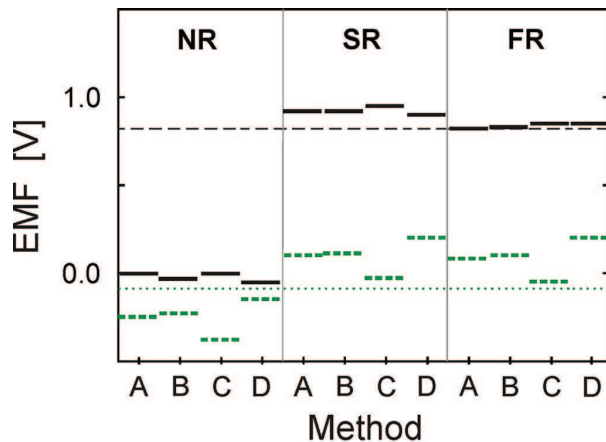


FIG. 3. Effect of relativity on the EMF of model-reaction, $M(s) + MO_2(s) \rightarrow 2MO(s)$, calculated with four different methods (A-D). Experimental values for $M=\text{Pb}$ (+0.82 V) and $M=\text{Sn}$ (-0.085 V) are indicated with the horizontal dashed and dotted lines, respectively. A) BAND (VWN), B) BAND (PBESol), C) BAND (PBESol-D), and D) FPLO (PW92). The level C has dispersion corrections.

are similar for Sn and Pb while the relativistic ones are not. Qualitatively, the tendency of Pb to be predominantly divalent can be related to the increased binding energy of the Pb 6s shell. Relativistic effects have also been suggested as responsible for the changing the structure of metallic lead from diamond to fcc[9, 27], as well being necessary to determine phase transitions between fcc, hcp, and bcc structures[10].

Moreover, it has been shown that the valence-shell relativistic effects of the Periodic Table scale roughly as Z^2 , Z being

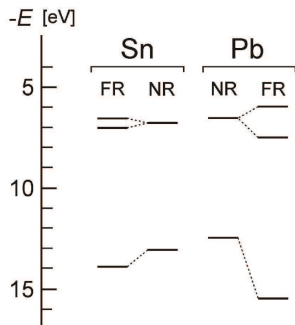


FIG. 4. Relativistic (FR) and non-relativistic (NR) Hartree-Fock orbital energies for the tin and lead atoms in their ns^2np^2 ground state. Note the relativistic stabilization of the ns level (lowest in the figure), leading to higher oxidative power for Pb(IV) than for Sn(IV). Data from Desclaux[28].

the full nuclear charge[8]. For tin and lead the ratio is

$$\left[\frac{Z(\text{Sn})}{Z(\text{Pb})} \right]^2 = \left[\frac{50}{82} \right]^2 = 0.372, \quad (6)$$

while the fully relativistic voltage changes, ΔE , calculated for the 'toy models'(5) yield

$$\left[\frac{\Delta E(\text{Sn})}{\Delta E(\text{Pb})} \right]^2 = \left[\frac{0.34V}{0.86V} \right]^2 = 0.395. \quad (7)$$

Indeed, the EMF calculated for the non-relativistic lead 'toy-model' is similar to the analogous tin model reaction, treated at fully-relativistic level. It also explains why the analogous reaction (1) for tin is unknown.

Concluding, the lead-acid battery belongs to those familiar phenomena, whose characteristic features are due to the relativistic dynamics of fast electrons when they move near a heavy nucleus. In this case the main actors are the 6s valence electrons of lead, in the substances involved. This insight may not help one to improve the lead battery, but it could be useful in exploring alternatives. Finally, we note that cars start due to relativity.

PP and PZE belong to the Finnish Center of Excellence in Computational Molecular Science (CMS) and used computer resources at CSC, Espoo, Finland. PZE acknowledges support

by Magnus Ehrnrooths Stiftelse and Finnish Cultural Foundation. RA, AB, and PL are grateful for time allocated on Swedish National Supercomputing facilities and for financial support from the Swedish Research Council (VR) and Formas Research Council.

* rajeev.ahuja@fysik.uu.se

† pekka.pyykkö@helsinki.fi

‡ patryk.ze@cornell.edu

- [1] G. Planté, C. R. Acad. Sci., **50**, 640 (1860).
- [2] P. Kurzweil, J. Power Sourc., **195**, 4424 (2010).
- [3] J. J. Esperilla, J. Félez, G. Romero, and A. Carretero, Simulat. Model. Pract. Theor., **15**, 82 (2007).
- [4] J. J. Esperilla, J. Félez, G. Romero, and A. Carretero, J. Power Sourc., **165**, 436 (2007).
- [5] J. C. Phillips, *Bonds and Bands in Semiconductors* (Academic Press, New York, 1973) see pp. 16-17.
- [6] J. P. Desclaux and P. Pyykkö, Chem. Phys. Lett., **29**, 534 (1974).
- [7] P. Pyykkö, Adv. Quantum Chem., **11**, 353 (1978).
- [8] P. Pyykkö, Chem. Rev., **88**, 563 (1988), see Fig. 11.
- [9] N. E. Christensen, S. Satpathy, and Z. Pawlowska, Phys. Rev. B, **34**, 5977 (1986).
- [10] A. Y. Liu, A. Garcia, M. L. Cohen, B. K. Godwal, and R. Jeanloz, Phys. Rev. B, **43**, 1795 (1991).
- [11] M. J. Verstraete, M. Torrent, F. Jollet, G. Zérah, and X. Gonze, Phys. Rev. B, **78**, 045119 (2008).
- [12] H. J. Terpstra, R. A. de Groot, and C. Haas, Phys. Rev. B, **52**, 11690 (1995).
- [13] U. Häussermann, P. Berastegui, S. Carlson, J. Haines, and J.-M. Leger, Angew. Chem. Int. Ed., **40**, 4624 (2001).
- [14] D. J. Payne, J. Mater. Chem., **17**, 267 (2007).
- [15] M. Heinemann, H. Terpstra, C. Haas, and R. A. de Groot, Phys. Rev. B, **52**, 11740 (1995).
- [16] D. J. Payne, Chem. Phys. Lett., **411**, 181 (2005).
- [17] D. J. Payne, J. El. Spectr. Rel. Phen., **169**, 26 (2009).
- [18] J. R. Anderson and A. V. Gold, Phys. Rev., **139**, A1459 (1965).
- [19] T. L. Loucks, Phys. Rev. Lett., **14**, 1072 (1965).
- [20] G. Planté, *Recherches sur l'Électricité de 1859 à 1879* (Gauthier-Villars, Paris, 1883).
- [21] J. A. Duisman and W. F. Giauque, J. Phys. Chem., **72**, 562 (1968).
- [22] <http://www.scm.com>, "Band2009.01 rev. 21855,".
- [23] K. Koepernik and H. Eschrig, Phys. Rev. B, **59**, 1743 (1999).
- [24] D. R. Lide, *CRC Handbook of Chemistry and Physics 74th Edition* (CRC Press, Boca Raton, 1993).
- [25] J. P. Perdew and Y. Wang, Phys. Rev. B, **45**, 13244 (1992).
- [26] A. Holleman and N. Wiberg, *Lehrbuch der Anorganischen Chemie, 101. Auflage*, edited by N. Wiberg (Walter de Gruyter, Berlin and New York, 1995) see p. 985.
- [27] A. Hermann, J. Furthmüller, H. W. Gäggeler, and P. Schwerdtfeger, Unpublished results.
- [28] J. P. Desclaux, At. Data Nucl. Data Tables, **12**, 311 (1973).